Journal of Applied Polymer Science

Magnetite/graphene/polyaniline composite for removal of aqueous hexavalent chromium

Dilip K. L. Harijan, Vimlesh Chandra
Department of Chemistry, Dr. Harisingh Gour University Sagar, Madhya Pradesh, India
Correspondence to: V. Chandra (E-mail: vchandg@gmail.com)

ABSTRACT: Here, we report the synthesis of Fe_3O_4/G/PANI composite containing magnetite nanoparticles (Fe_3O_4), graphene sheets (G), and polyaniline (PANI) via chemical route for removal of toxic Cr (VI) from water. TEM image shows the formation of uniformly distributed magnetite nanoparticles on graphene/PANI composite. HRTEM images shows the formation of crystalline magnetite nanoparticles showing lattice fringes with inter-planner distance 0.21 nm. The magnetic measurement shows magnetization 22 emu/g and ferromagnetic property of the adsorbent. The equilibrium adsorptions were well-described by the Langmuir isotherm model and shows maximum adsorption capacity 153.54 mg/g at pH 6.5 and temperature 30 °C. The kinetics data well fitted by pseudo-second-order model and around 86% Cr (VI) removal completed within 20 min. The Cr (VI) removal capacitive decreases with increase in pH and ionic strength. The adsorbent shows leaching of iron nanoparticles at pH 1 whereas stable in solution having pH 2 and more. © 2016 Wiley Periodicals, Inc. J. Appl. Polym. Sci. **2016**, *133*, 44002.

KEYWORDS: adsorption; conducting polymers; magnetism and magnetic properties

Received 20 February 2016; accepted 1 June 2016
DOI: 10.1002/app.44002

INTRODUCTION

Industrial revolution and fast urbanization has led to an increased release of wastewater containing chromium in the water. In aquatic system, chromium metal exists mainly in the two oxidation states such as Cr (III) and Cr (VI). Cr (III) is an essential element needed to humans and less toxic and immobile than Cr (VI).[1] Chromium (VI) exist in the water mainly as dichromate ($Cr_2O_7^{2-}$), chromate (CrO_4^{2-}), and hydrogen chromate ($HCrO_4^-/H_2CrO_4$) at pH equal to, less than, and above 6.8, respectively.[2] The US Environmental Protection Agency (EPA) and World Health Organization (WHO) recommended that a maximum allowable chromium concentration in drinking water should not be higher than 0.1 mg/L and 0.05 mg/L, respectively. On drinking water more than the permissible limit for prolonged period can lead to skin irritation, lung cancer, and damage to kidney, liver, and gastrointestinal track.[3] Hexavalent chromium concentration has to be reduced to permissible limit before discharging industrials effluents to aquatic environment.[4]

Polyaniline (PANI) is a conducting polymer and has high removal capacity toward hexavalent chromium anions.[5] The conjugated PANI has three different structures, i.e., leucoemeraldine (LB), emeraldine (EB), and pernigraniline (PB).[6] It has good reduction behaviors for Cr (VI) to Cr (III) with the electron transfer from the LB or EB states to PB state.[7] PANI in powder form is a good candidate for highly efficient Cr (VI) removal due to high adsorption capacity, low cost, and easily bulk production.[8–10] PANI is macroporous in nature and has small surface area and has been used for adsorption of Cr (VI). PANI doped with sulfuric acid shows maximum Cr (VI) removal 95.79 mg g^{-1}.[11] PANI has been functionalized with sawdust,[12] silica gel,[13] ethyl cellulose,[14] and polyacrylonitrile[15] to enhance Cr (VI) removal capacity.

The most recent discovered synthetic allotrope of carbon, two dimensional graphene and its derivatives have been used in water treatment containing organic, inorganic, and biological pollutants.[16–18] Graphene-based magnetic adsorbents have been widely accepted for treatment of contaminated water due to low operation cost and do not need membrane and electrical/solar energy.[19] Fe_3O_4 hollow microspheres/graphene oxide (GO) composite showed sorption capacity for Cr (VI) 32.33 mg g^{-1}.[20] Three-dimensional magnetic GO foam/Fe_3O_4 composite exhibited high Cr (VI) adsorption capacity of 258.6 mg g^{-1}.[21] The reduced GO-Fe_3O_4 composite was fabricated having size around 10 nm via solvothermal process which showed Cr (VI) adsorption capacity 5.5 mg g^{-1} at neutral pH.[22] In this article, we

Additional Supporting Information may be found in the online version of this article.

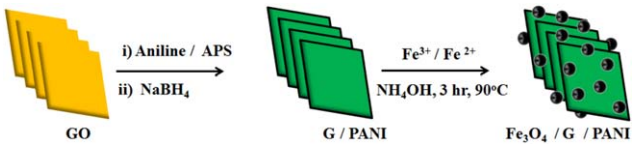

Figure 1. Synthesis of Fe_3O_4/G/PANI composite via chemical route. [Color figure can be viewed in the online issue, which is available at wileyonlinelibrary.com.]

report the synthesis of Fe_3O_4/G/PANI composite via chemical route for removal of aqueous Cr (VI) (Figure 1).

EXPERIMENTAL

Chemicals

Graphite (Alfa Aesar, Massachusetts United States), Sodium Nitrate (Merck, Mumbai India), Potassium Permanganate (Aldrich, Bangalore India), Hydrogen Peroxide (30 wt % Alfa Aesar, Heyshan England), Sulfuric Acid (Merck, Mumbai India), Hydrochloric Acid (Merck, Mumbai India), Ferric Chloride Hexahydrate (Merck, Mumbai India), Ferrous Chloride Tetrahydrate (Merck, Mumbai India), Liquor ammonia (Merck, Mumbai India), Aniline (Merck, Mumbai India), Ammonium Persulphate (Sigma Aldrich, Bangalore India) were obtained and used for synthesis of adsorbents and potassium dichromate (Merck, Mumbai India) in making chromium contaminated water.

Synthesis of Graphene Oxide

GO was synthesized via chemical oxidation of graphite as reported earlier.[23] Approximately 5 g graphite and 5 g $NaNO_3$ were added in 125 mL of H_2SO_4 (95%) in a 1000-mL flask at ice temperature. The mixture was stirred for 30 min at this temperature. Approximately 15 g potassium permanganate was added to the suspension very slowly and temperature was maintained below 15 °C. After this, ice bath was removed and the mixture was stirred at 35 °C until it became brownish paste and then diluted with slow addition of 250 mL water. Further, this solution was diluted by adding 500 mL water and 10 mL H_2O_2 (30 wt %). The solution mixture was washed with 10% HCl many times to remove metal impurities of graphite and finally washed with the deionized (DI) water several times. After filtration and drying under vacuum and at room temperature, the GO was obtained as a powder.

Synthesis of Graphene-Polyaniline Composite

About 200 mg of GO and 2 mL aniline were dispersed in 100 mL of 1 *M* HCl aqueous solution at 0 °C. About 5 g ammonium persulfate was dissolved in 100 mL of 1 *M* HCl and cooled down to 0 °C. Polymerization of aniline was carried out by addition of ammonium persulfate in the aniline solution with continuous stirring at ice temperature and resulting solution was allowed to stand at room temperature for overnight. The product was washed with copious amount of water and redispersed into 100 mL water. The reduction of GO was carried out using 10 mL of 0.5 *M* sodium borohydride solution. The product was washed with water and finally with ethanol and dried at 100 °C for 10 h.

Synthesis of Fe_3O_4 and Fe_3O_4/G/PANI Composite

Approximately 232 mg G/PANI composite was dispersed in 50 mL distilled water and mixed solution of ferric chloride hexahydrate ($FeCl_3.6H_2O$, wt = 1.3515 g) and ferrous chloride tetrahydrate ($FeCl_2.4H_2O$, wt = 0.4971 g) in 25 mL water was added with continuous mechanical stirring. The temperature raised to 90 °C and the required amount of 1 *M* NaOH aqueous solution was added to reaction mixture slowly to maintain pH = 10. After 2 h, the suspension was cooled down to room temperature and black color product was separated by magnet and washed with distilled water. The protonation of the adsorbent was carried out by washing with excess amount of 2 *M* HCl solution and dried at 100 °C. The synthesis of magnetite nanoparticles was carried out using the same way but in the absence of G/PANI.

Cr (VI) Adsorption Experiments

A stock solution of initial concentration (C_o) 100 ppm was prepared in distilled water by dissolving 282 mg of potassium dichromate ($K_2Cr_2O_7$, F.W. 294.19) in 1L and pH 6.5. The pH of solution was maintained using HCl and NaOH solution. The required amount of adsorbent was added to Cr (VI) solution and mechanically stirred for different time interval. At the end of adsorption experiment, the adsorbent was separated from solution using hand held magnet. The Cr (VI) concentration in the solution after (C) adsorption was measured using UV–vis spectrophotometer by monitoring the absorbance change at maximum wavelength ($\lambda_{max} \sim 372$ nm). The equilibrium adsorption capacity was calculated q (mg g^{-1}) = $(C_o - C) \times V/w$, where w is adsorbent dose (mg) and V (mL) volume of Cr (VI) solution.

Analysis Instruments

The powder X-ray diffraction patterns (XRD) were recorded on a Bruker with Cu-K_α irradiation ($\lambda = 1.5406$ Å). Fourier transformed infrared (FTIR) spectra were recorded using a Bruker Tensor 37. The microscopic features of the samples were characterized by transmission and high resolution transmission electron microscopy (TEM and HRTEM) using FEI Tecnai G2F30 S-Twin with an accelerating voltage of 200 kV. The magnetic properties were studied using vibrating sample magnetometer, EV-7, ADE DMS magnetic, USA. UV-visible spectra of the samples were obtained using a Systronics spectrometer in the wavelength region between 200 and 800 nm.

RESULTS AND DISCUSSION

The TEM observation of G/PANI shows the formation of PANI on the surface of graphene sheets due to π–π interaction and adopts morphology similar to the graphene sheet [Figure 2(a)]. Fe_3O_4/G/PANI composite shows magnetite nanoparticles coated with G/PANI and distributed uniformly [Figure 2(b,c)]. The crystallite size of Fe_3O_4 nanoparticles is around 12 nm which is in good agreement with Debye Scherrer calculation. HRTEM image shows the formation of lattice fringes with inter-planner distance 0.21 nm which corresponds to (400) plane of the magnetite phase. The powder X-ray diffraction patterns of graphite shows a sharp diffraction peak at 26.5° corresponding to (002) plane (Supporting Information Figure SI-1). On oxidation of graphite using oxidizing agents, the inter-planer distance between (002) planes increases due to intercalations of different functional groups and peak shifted to lower angle $2\theta = 14.6°$. Fe_3O_4/G/PANI composite shows peaks at 2θ equal to 18.6°, 30.2°, 35.26°, 43.0°, 54.2°, 57.44°, and 62.5° corresponds to spinel phase of Fe_3O_4

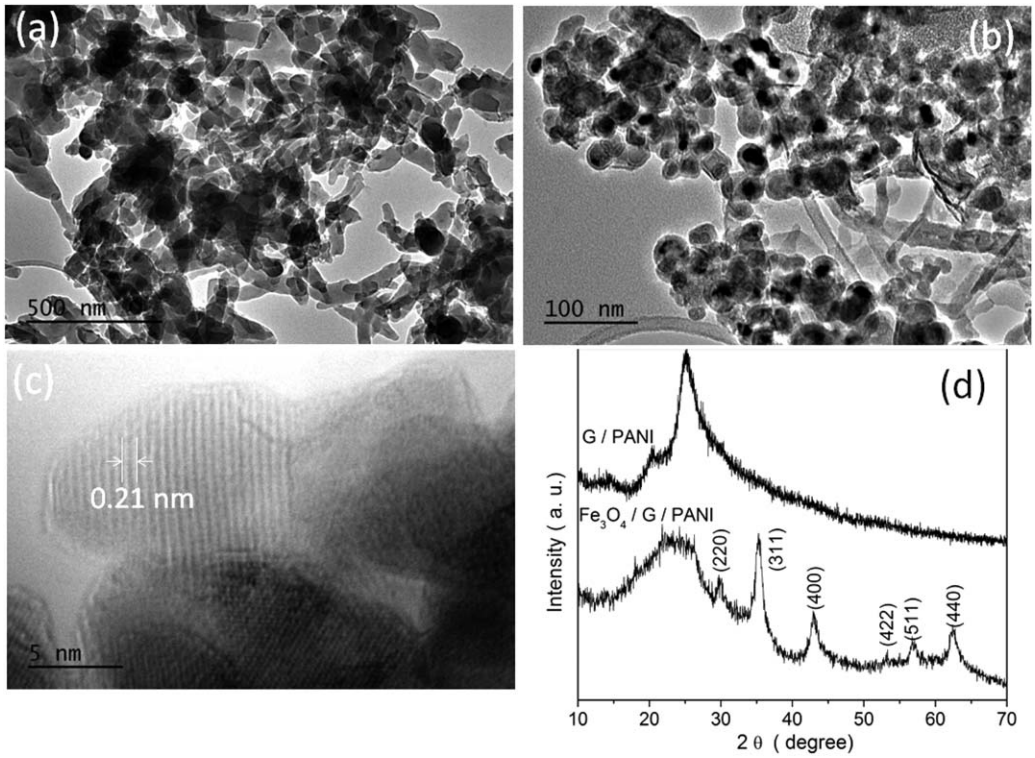

Figure 2. TEM image of (a) G/PANI, (b) Fe_3O_4/G/PANI, (c) HRTEM image of Fe_3O_4/G/PANI, (d) X-ray diffraction patterns of G/PANI and Fe_3O_4/G/PANI.

(JCPDS No. 75-0033), The crystallite size calculated from Debye Scherrer formula shows 12 nm. The broad peak at $2\theta = 25°$ is due to the formation of amorphous G/PANI.

Fourier transform Infrared (FTIR) spectrum was recorded to study nature of functional groups (Supporting Information Figure SI-2). The FTIR spectra of GO shows carbonyl C═O (1719 cm^{-1}), aromatic C═C (1620 cm^{-1}), carboxyl O═C—O (1356 cm^{-1}), epoxy C—O (1217 cm^{-1}), and alkoxy C—O (1049 cm^{-1}) stretching vibrational modes. The reduction of GO to graphene shows two peaks at 1555 and 1182 cm^{-1} which correspond to the aromatic C═C stretch and C—O stretch, respectively. The Fe_3O_4/G/PANI composite shows aromatic C—C stretching vibrations bands around 1570 and 1468 cm^{-1} corresponding to the quinoid and benzenoid ring, respectively. The peak at 1291 cm^{-1} is related to the C—N stretching vibration of benzenoid unit. The broad and strong peak around 1133 cm^{-1} is due to the vibrational mode of N═Q═N, where Q refers to quinonic type rings. A band at about 798 cm^{-1} could be attributed to the C—H out-of-plane deformation vibrations, while the many low-intensity peaks ranging from 780 to 580 cm^{-1} can be assigned to the vibrations of the C—H bonds in the benzene rings. The band around 598 cm^{-1} corresponds to intrinsic vibration of the tetrahedral voids of Fe_3O_4.[24]

The magnetic measurement of Fe_3O_4/G/PANI composite and Fe_3O_4 was carried out using vibrating sample magnetometer at room temperature (30 °C) as shown in Figure 3(a). The *M* vs. *H* plot shows decrease in magnetization of Fe_3O_4 nanoparticles from 53 emu/g to 22 emu/g (Fe_3O_4/G/PANI). The decrease in magnetization originates from the nonmagnetic nature of G/PANI. The magnetization from this work has been found comparable to previous report in literature (Supporting Information Table SI-1). The magnetization versus applied magnetic field shows hysteresis loop at room temperature indicates formation of ferromagnetic nature of the composite. The magnetic hysteresis loop shows decrease in coercivity with PANI loading due to reduction in anisotropic property of magnetite particles (Supporting Information Figure SI-3). The aqueous solution of Cr (VI) and adsorption onto Fe_3O4/G/PANI and separation of adsorbent using hand held magnet is shown in Figure 3(b–d).

Hexavalent Chromium Adsorption

The Cr (VI) adsorption onto PANI, graphene, magnetite, G/PANI, and Fe_3O_4/G/PANI was studied at pH 6.5, temperature 30 °C, adsorbent dose 0.5 mg/mL, Cr (VI) concentration 100 ppm, and time of adsorption 2 h [Figure 4(a)]. The adsorption of Cr (VI) on pure graphene sheets, Fe_3O_4, and PANI are 1.0 mg/g, 7 mg/g, and 96 mg/g, respectively. The G/PANI shows Cr (VI) adsorption capacity higher than the PANI. The increase in the Cr (VI) removal capacity originates from the presence of graphene sheets having high surface area and electron transport and enhances adsorptive sites and electroreductive capacitance of the PANI. The Fe_3O_4/G/PANI composite shows poor Cr (VI) removal capacity compared to the G/PANI mainly comes from low surface area and weak adsorptive behavior of magnetite nanoparticles but makes adsorbent magnetic in nature.

Effect of Adsorption Time. The time-dependent adsorption of Cr (VI) on to Fe_3O_4/G/PANI was studied for 50 ppm, 75 ppm, and 100 ppm Cr (VI) solution at pH =6.5 and $T = 30$ °C and adsorbent dose 0.5 mg/mL. The time dependent results showed

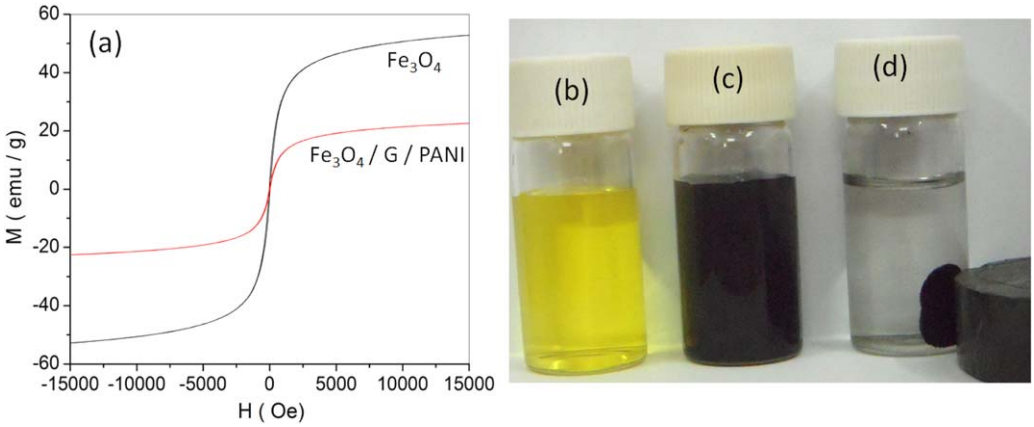

Figure 3. (a) Magnetization (M) vs. applied magnetic field (H) plot of Fe_3O_4/G/PANI and Fe_3O_4 at 300 K, (b) 50 ppm Cr (VI) solution, (c) dispersion of adsorbent, and (d) separation of adsorbent using magnet after Cr (VI) adsorption. [Color figure can be viewed in the online issue, which is available at wileyonlinelibrary.com.]

that adsorption capacity increases with increase in contact time and attained equilibrium after 40 min [Figure 4(b)]. The data was analyzed according to pseudo-first-order kinetics and second-order kinetics models expressed as follows:

$$\text{Pseudo-first-order kinetics: } \ln(q_e - q_t) = \ln q_e - k_1 t \qquad (1)$$

$$\text{Pseudo-second-order kinetics: } \frac{1}{q_t} = \frac{1}{q_e^2 k_2} + \frac{1}{q_e} t \qquad (2)$$

where q_t and q_e are the amounts (mg/g) of Cr (VI) adsorbed at time t and at equilibrium, respectively, k_1 (min^{-1}) and k_2 (g/mg min) are the equilibrium rate constant of pseudo-first

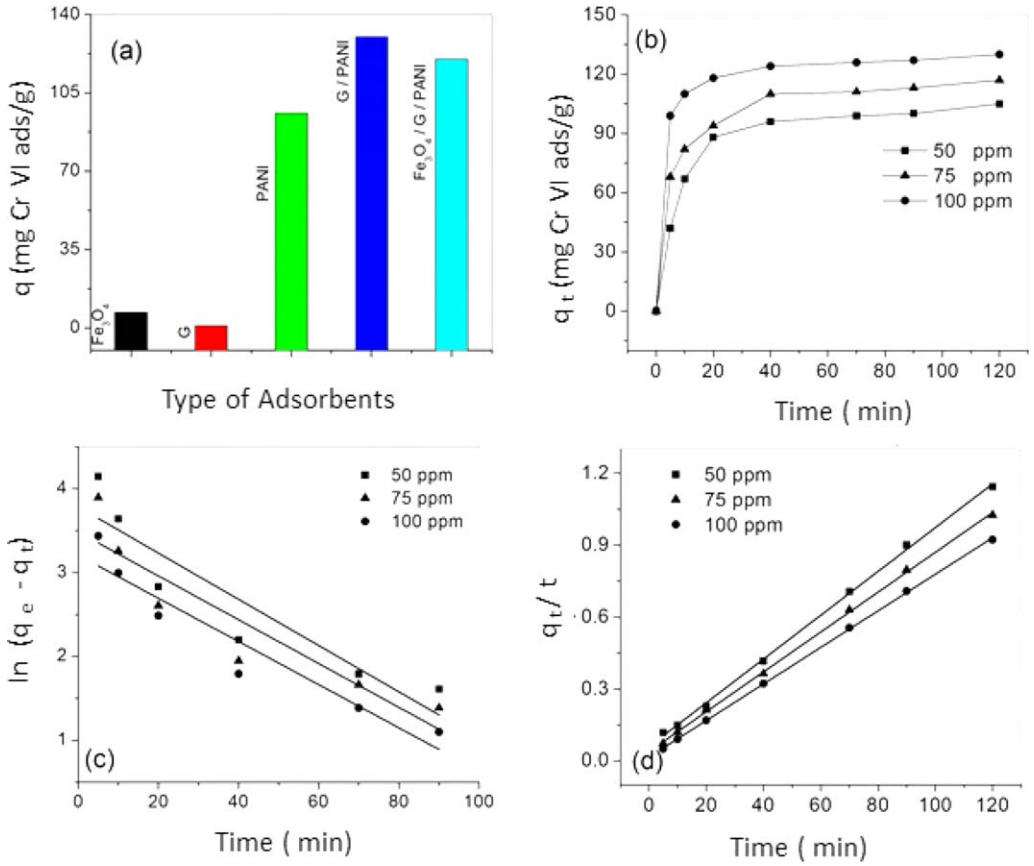

Figure 4. (a) Cr (VI) adsorption on graphene (G), magnetite (Fe_3O_4), PANI, G/PANI, and Fe_3O_4/G/PANI, (b) time dependent adsorption of Cr (VI) onto Fe_3O_4/G/PANI, (c) linear fit for pseudo first order kinetics, and (d) pseudo-second-order kinetics. [Color figure can be viewed in the online issue, which is available at wileyonlinelibrary.com.]

Table I. Kinetics Study for Cr (VI) Adsorption onto Fe_3O_4/G/PANI Composite

Initial Cr (VI) concentration	Pseudo-second-order kinetics			Pseudo-first order kinetics		
	q_e	k_2	R^2	q_e	k_1	R^2
50	111.11	1.35×10^{-3}	0.9982	43.12	2.75×10^{-2}	0.8200
75	120.34	1.76×10^{-3}	0.9996	32.45	2.61×10^{-2}	0.8095
100	131.20	3.56×10^{-3}	0.9997	24.67	2.51×10^{-2}	0.8936

and second-order adsorption. The kinetic data did not fit well with pseudo-first-order [Figure 4(c)] however pseudo-second-order kinetics model fitted well [Figure 4(d)]. The different parameters were calculated and presented in Table I.

Intraparticle diffusion model is described using the equation:

$$q_t = k_p t^{0.5} + C \tag{3}$$

where k_p is the intraparticle diffusion constant (mg/g $min^{0.5}$). The plot of q_t vs. $t^{0.5}$ (Supporting Information Figure SI-4) does not show straight line passing through origin hence resultant adsorption kinetics does not govern interparticle diffusion model.

Effect of Initial Concentration. The role of initial concentration of Cr (VI) was studied by changing concentration from 40 ppm–100 ppm, at pH = 6.5, $T = 30\,^{\circ}C$ and adsorbent dose = 0.5 mg/mL [Figure 5(a)]. The adsorption capacity increases with increase in the initial concentration.

The isotherm was fitted with Langmuir and Freundlich model.

The Langmuir isotherm is expressed as

$$q_e = \frac{abC_e}{1 + bC_e} \tag{4}$$

and Freundlich isotherm is represented by

$$q_e = k_F (C_e)^{1/n} \tag{5}$$

where a is the maximum adsorption capacity (mg g^{-1}), b is the constant related to the affinity of the active binding sites (l/mg), k_F is the binding constant and depends on the relative adsorption capacity of the adsorbent (mg g^{-1}), and $(1/n)$ is the adsorption intensity.

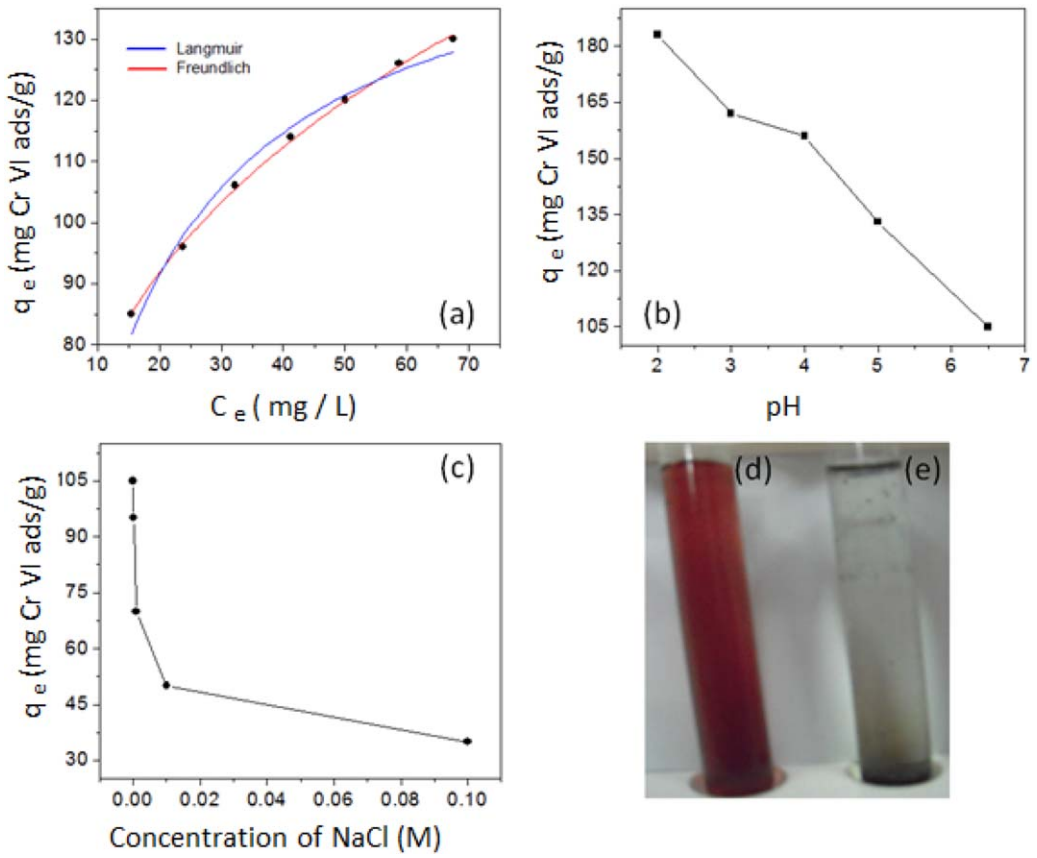

Figure 5. (a) The isotherms curves fitted with Freundlich (red) and Langmuir (blue), (b) role of solution Ph, and (c) effect of sodium chloride on Cr (VI) adsorption on Fe_3O_4/G/PANI, (d) formation of Fe^{3+}-salicylic acid coloured complex, and (e) Leaching of iron nanoparticles from composite in 1 *M* HCl after 172 h. [Color figure can be viewed in the online issue, which is available at wileyonlinelibrary.com.]

Table II. Langmuir and Freundlich Adsorption Isotherm Parameters for Chromium Removal onto Fe_3O_4/G/PANI

Isotherm type	Isotherm const.	Fe_3O_4/G/PANI
Langmuir	a (mg/g)	153.54
	b (l/mg)	0.0731
	R^2	0.9873
Freundlich	k_F	38.40
	n	3.45
	R^2	0.9984

The results show correlation factor R^2 higher for Freundlich model (=0.9984) compared to the Langmuir (0.9873). This suggests adsorption of Cr (VI) onto the adsorbent governed by the multilayers formation. The maximum adsorption capacity (q_{max}) was found 153.54 mg/g and other parameter are given in Table II.

Effect of Solution pH. The Cr (VI) adsorption found pH dependent and studied in the pH range of 2–12, initial Cr (VI) 100 ppm, temperature 30 °C, and adsorbent dose 0.5 mg/mL as shown in Figure 5(b). The adsorption was found maximum 182 mg/g at pH 2 and decreases with increase in pH of the solution. Hexavalent chromium exists in the aqueous solution as bichromates ($HCrO_4^-$) in the range of pH 2–6. The decrease in pH enhances the positive charge on the surface of adsorbent ($-NH_3^+$) which enhances electrostatic interaction between anions $HCrO_4^-$ and adsorbent. The reduction of Cr (VI) to Cr (III) in the acidic medium on the surface of adsorbent governed by the following equation.[25]

$$HCrO_4^- + 7\ H^+ + 3e \rightarrow Cr^{3+} + 4H_2O \quad (6)$$

The electrons for the reduction of Cr (VI) to Cr (III) are supplied from amino groups of PANI. The presence of graphene sheets on the surface of PANI enhanced electron donation capacity and results in the increased reduction process of Cr (VI) to Cr (III). The Cr (III) exists as Cr^{3+} and Cr $(OH)^{2+}$ in the solution and does not precipitate as Cr $(OH)_3$ in the solution having pH less than 6 and forms tridentate and bidentate coordination bonds with nitrogen atoms of the adsorbent.[26]

Effect of Ionic Strength. The effect of ionic strength on the removal of chromium (VI) was studied at pH 6.5, initial Cr (VI) concentration 100 ppm, temperature 30 °C, and adsorbent dose 0.5 mg/mL [Figure 5(c)]. The adsorption capacity of Cr (VI) on adsorbent decreases with increase in the concentration of sodium chloride. This decrease in adsorption is due to the dominating effect of Cl^{-1} ions.[27] The adsorption results indicate that when the concentration of NaCl was increased from 0 to 10^{-1} M there was around 67.6% decrease in adsorption capacity.

The desorption of the bound Cr (VI) ions was studied using different pH solution for regeneration of adsorbent. The desorption capacities of Fe_3O_4/G/PANI at pH 2, 4, and 12 are 2%, 16%, and 70%, respectively. The iron metal leaching from composite was studied by adding 30 mg of it in 10 mL of hydrogen chloride (HCl) solution of pH 1–5. The iron metal leaching started within 24 h in the solution of pH 1 [Figure 5(e)]; however there was no metal leaching observed for acid solution of pH 2–5 even after 170 h. The presence of Fe^{3+} ion in the solution was tested by adding 0.002 M salicylic acid which formed colored complex in case of pH = 1 and remain colorless for pH 2–5 [Figure 5(d)]. These results indicate that the composite is stable in the acidic medium of pH 2–5.

CONCLUSIONS

The magnetic adsorbent (Fe_3O_4/G/PANI) was synthesized via chemical route. The presence of G/PANI composite on the surface of magnetite nanoparticles removed around 86% Cr (VI) within 20 min from 100 ppm solution at pH = 6.5. The Cr (VI) removal is the combined effect of electrostatic interaction and electroreduction and comes from amino groups of PANI. The adsorption data well fitted with Langmuir and Freundlich with maximum adsorption capacity 153.54 mg g^{-1}. More than 70% Cr (VI) ions can be easily desorbed from the adsorbent using basic solution of pH = 12. The leaching of iron metal from adsorbent was tested and showed stability in the pH = 2– 6 and unstable in pH = 1.

ACKNOWLEDGMENTS

V. Chandra thank for the financial support of University Grant Commission (UGC Start-up Grants-BSR N. F 30/2/2014) and Sophisticated Instruments Center (SIC) and Department of Chemistry at Dr. Harisingh Gour University for different characterization/measurements of the samples.

REFERENCES

1. Li, Q.; Sun, L.; Zhang, Y.; Qian, Y.; Zhai, J. *Desalination* **2011**, *266*, 188.
2. Mohan, D.; Pittman, C. U., Jr. *J. Hazard. Mater. B* **2007**, *137*, 762.
3. Torresdey, J. L. G.; Gonzalez, J. H.; Tiemann, K. J.; Rodriguez, O.; Gamez, G. *J. Hazard. Mater.* **1998**, *57*, 29.
4. Wang, X. S.; Tang, Y. J.; Chen, L. F.; Li, F. Y.; Wan, W. Y.; Tan, Y. B. *Clean—Soil Air Water* **2010**, *38*, 263.
5. Olad, A.; Nabavi, R. *J. Hazard. Mater.* **2007**, *147*, 845.
6. Ogoshi, T.; Hasegawa, Y.; Aoki, T.; Ishimori, Y.; Inagi, S.; Yamagishi, T. *Macromolecules* **2011**, *44*, 7639.
7. Farrell, S. T.; Breslin, C. B. *Environ. Sci. Technol.* **2004**, *38*, 4671.
8. Chiou, N. R.; Epstein, A. J. *Adv. Mater.* **2005**, *17*, 1679.
9. Guo, X.; Fei, G. T.; Su, H.; Li, D. Z. *J. Phys. Chem. C* **2011**, *115*, 1608.
10. Huang, J.; Kaner, R. B. *Chem. Commun.* **2006**, 367.
11. Zhang, R.; Ma, H.; Wang, B. *Ind. Eng. Chem. Res.* **2010**, *49*, 9998.
12. Ansari, R. *Acta Chim. Slov.* **2006**, *53*, 88.

13. Karthik, R.; Meenakshi, S. *J. Water Process. Eng.* **2014**, *1*, 37.
14. Qiu, B.; Xu, C.; Sun, D.; Yi, H.; Guo, J.; Zhang, X.; Qu, H.; Guerrero, M.; Wang, X.; Noel, N.; Luo, Z.; Guo, Z.; Wei, S. *ACS Sustain. Chem. Eng.* **2014**, *2*, 2070.
15. Wang, J.; Pan, K.; Giannelis, E. P.; Cao, B. *RSC Adv.* **2013**, *3*, 8978.
16. Sreeprasad, T. S.; Maliyekkal, S. M.; Lisha, K. P.; Pradeep, T. *J. Hazard. Mater.* **2011**, *186*, 921.
17. Perreault, F.; de Faria, A. F.; Elimelech, M. *Chem. Soc. Rev.* **2015**, *44*, 5861.
18. Kemp, K. C.; Seema, H.; Saleh, M.; Le, N. H.; Mahesh, K.; Chandra, V.; Kim, K. S. *Nanoscale* **2013**, *5*, 3149.
19. Humera, J.; Chandra, V.; Jung, S.; Lee, J. W.; Kim, K. S.; Kim, S. B. *Nanoscale* **2011**, *3*, 3583.
20. Wu, Y.; Ma, X.; Feng, M.; Liu, M. *J. Hazard. Mater.* **2008**, *159*, 380.
21. Lei, Y.; Chen, F.; Luo, Y.; Zhang, L. *J. Mater. Sci.* **2014**, *49*, 4236.
22. Harijan, D. K. L.; Chandra, V. *Environ. Prog. Sustain. Energ.* **2016**, *35*, 700.
23. Hummers, W. S.; Offeman, R. E. *J. Am. Chem. Soc.* **1958**, *80*, 1339
24. Waldron, R. D. *Phys. Rev.* **1955**, *99*, 1727.
25. Cimino, G.; Passerini, A.; Toscano, G. *Water Res.* **2000**, *34*, 2955.
26. Kumar, P. A.; Ray, M.; Chakraborty, S. *J. Hazard. Mater.* **2007**, *143*, 24.
27. Toledo, B.; Utrilla, J. R.; Garcia, M. A. F.; Castilla, C. M. *Carbon* **1994**,*32*, 93.